Available online at www.sciencedirect.com
SCIENCE DIRECT®
C. R. Chimie 7 (2004) 351–361
COMPTES RENDUS CHIMIE

Full paper / Mémoire

Application of the through-bond correlation NMR experiment to the characterization of crystalline and disordered phosphates

Franck Fayon [a,*], Ian J. King [b], Robin K. Harris [b], John S.O. Evans [b], Dominique Massiot [a]

[a] *Centre de recherche sur les matériaux à haute température, CNRS, 1D, av. de la Recherche-Scientifique, 45071 Orléans cedex 2, France*
[b] *Department of Chemistry, University of Durham, Durham DH1 3LE, UK*

Received 27 May 2003; accepted 28 October 2003

Available online 9 April 2004

Abstract

Through-bond correlation NMR experiments have been used to characterize the structure of MP_2O_7 crystalline compounds and disordered phosphates. For MP_2O_7 materials, the refocused INADEQUATE experiment allows discrimination between the possible space group symmetries of the room temperature structure. The results show that the room temperature structure of ZrP_2O_7 adopts *Pbca* symmetry. For lead phosphate glasses, the refocused INADEQUATE experiment can be used to determine the P–O–P through-bond connectivities between the different types of PO_4 tetrahedra. In these glasses, a correlation between the distributions of *J*-couplings and ^{31}P isotropic chemical shifts is shown by using the 2D J-resolved experiment. ***To cite this article: F. Fayon et al., C. R. Chimie 7 (2004).***

Résumé

Nous avons utilisé des techniques RMN de corrélation homonucléaire pour caractériser la structure de composés MP_2O_7 et de verres $PbO–P_2O_5$. L'expérience INADEQUATE refocalisé permet de discriminer les différents groupes d'espace possibles des composés MP_2O_7. Les résultats indiquent que ZrP_2O_7 adopte la symétrie *Pbca* à température ambiante. Pour les verres $PbO–P_2O_5$, l'expérience INADEQUATE refocalisée permet de déterminer les connectivités chimiques P–O–P entre les différents types de tétraèdres PO_4. Dans ces verres, une corrélation entre les distributions de couplage *J* et de déplacement chimique isotrope de ^{31}P est mise en évidence par des expériences 2D d'écho de spin. ***Pour citer cet article : F. Fayon et al., C. R. Chimie 7 (2004).***

Keywords: NMR; INADEQUATE; *J* coupling; Structure; MP_2O_7; Glasses

Mots clés : RMN ; INADEQUATE ; Couplage *J* ; Structure ; MP_2O_7 ; Verres

* Corresponding author.
E-mail address: fayon@cnrs-orleans.fr (F. Fayon).

doi:10.1016/j.crci.2003.10.019

1. Introduction

Over the last few years, various solid-state magic angle spinning NMR experiments have been proposed to determine the atomic connectivities in solids [1–12]. In rigid solids, the dipolar interactions are usually several orders of magnitude larger than the scalar *J* couplings. A large number of methods have been thus developed to reintroduce the through-space dipolar interaction under magic angle spinning (MAS), leading to the observation of nearest-neighbour spatial proximities in two-dimensional (2D) correlation spectra [1–7]. However, it has been recognised for several years that weak *J*-couplings can be used to obtain through-bond correlation spectra in rigid solids, providing a direct identification of atomic connectivities [8–12]. Recently, we have shown that the refocused INADEQUATE experiment allows a straightforward determination of the through-bond P–O–P connectivities in crystalline and disordered phosphates [13]. In this work, we illustrate the applications of the refocused INADEQUATE experiment to the structural characterisation of MP_2O_7 crystalline compounds (M = Zr, Sn) and lead phosphate glasses.

ZrP_2O_7 belongs to the $M^{4+}P_2O_7$ family of compounds that are of interest because several members of the family show low or negative coefficients of thermal expansion [14,15]. At high temperature, these compounds usually have a simple cubic structure, with $Z = 4$ and space group symmetry $Pa\bar{3}$, which can be described as a network of corner-sharing MO_6 octahedra and P_2O_7 pyrophosphate groups [15]. In this ideal cubic structure, the P_2O_7 groups are on 3-fold axes with the P–O–P bridging oxygen atoms at inversion centres, constraining by symmetry the P–O–P bond angles to 180°. At low temperature, these energetically unfavourable linear bond angles are partially or completely avoided by distortion of the ideal cubic structure, resulting in a room temperature structure with a tripled (3 × 3 × 3) unit cell ($Z = 108$) [15–17]. Assuming phase transitions with group sub-group relationship, symmetry considerations indicate that the room temperature structure can adopt one of 12 possible space groups derived from the symmetry ($Pa\bar{3}$) of the ideal high temperature phase [15]. These various space group symmetries give rise to very subtle differences in the reflections observed by powder X-ray diffraction, but, as the symmetry of the possible space group is lowered, the number of crystallographically distinct P sites and the number of different types of P_2O_7 groups in the asymmetric unit dramatically increases (see Table 1). As previously demonstrated in the case of SiP_2O_7 [18] and TiP_2O_7 [19], through-bond correlation NMR methods, which allow the determination of the number of independent P sites in the asymmetric unit and the phosphorus connectivity scheme, can be used to discuss the possible space groups adopted at room temperature by these materials.

Table 1
Number of different types of $P_2O_7^{4-}$ groups and number of unique crystallographic P sites expected for the possible space group symmetries adopted at room temperature by MP_2O_7 materials [15,35]

Space group	No. of P_2O_7 groups with two equivalent P sites	No. of P_2O_7 groups with two inequivalent P sites	No. unique P sites
$Pa\bar{3}(1 \times 1 \times 1)$	1		1
$Pa\bar{3}$	1	5	11
$P2_13$		11	22
$R\bar{3}$	2	18	38
$R3$		38	76
$Pbca$	1	13	27
$Pca2_1$		27	54
$P2_12_12_1$		27	54
$P2_1/c$	2	26	54
Pc		54	108
$P2_1$		54	108
$P\bar{1}$	4	52	108
$P1$		108	216

In the case of phosphate glasses, magic-angle-spinning NMR provides evidence of the basic building units of the disordered network [20]. The various PO_4 tetrahedral units (Q^n with n: number of bridging oxygen atoms per tetrahedron) are usually partly resolved in 1D MAS spectra, depending on glass composition. Dipolar correlation techniques have been used to probe the spatial proximities of these Q^n units, from which the Q^n pair connectivities were deduced [21–23]. The refocused INADEQUATE experiment, which proves to be very useful for crystalline materials, can also be applied to obtain through-bond correlation spectra in phosphate glasses, allowing characterization of the different Q^n units and their connectivities in the disordered network.

2. Experimental

2.1. Synthesis

High-purity crystalline ZrP_2O_7 was prepared from $ZrOCl_2$ and H_3PO_4 (85%), which were mixed in a 2:1 molar ratio in a platinum crucible and heating to 350 °C for 1 h. The resultant powder was washed with distilled water, and heated to 750 °C then 1000 °C for a 12-h period. The high purity of the ZrP_2O_7 sample was confirmed by X-ray and neutron powder diffraction.

The $PbO_x(P_2O_5)_{1-x}$ glasses (x = 0.52, 0.59, 0.66) were prepared from reagent-grade PbO and $(NH_4)_2HPO_4$. The glass samples were melted in Pt crucibles for 1 h under air at temperatures varying from 700 to 850 °C depending on composition and quenched by partly immersing the crucible in water. Glass compositions were checked by microprobe (1 mol% uncertainties).

2.2. Solid-state NMR

The solid-state NMR experiments were performed at room temperature on a Bruker DSX 300 spectrometer (7.0 T) with a 4-mm MAS probehead operating at a Larmor frequency of 121.4 MHz for ^{31}P. The one-dimensional (1D) ^{31}P MAS spectra of the crystalline and glassy samples were recorded at various spinning frequencies (from 3 to 15 kHz) using single-pulse (π/8) acquisition. The recycle delay varied from 80 to 20 s for the crystalline sample and the glasses, respectively, to ensure no saturation.

The two-dimensional (2D) ^{31}P through-bond single-quantum-double-quantum (SQ–DQ) MAS NMR correlation spectra were acquired using the refocused INADEQUATE [24] sequence [12] (Fig. 1a). The π/2 pulse duration was 2.3 μs. The delay τ in the excitation and reconversion periods was synchronized with the rotor period and was set to 10 ms for ZrP_2O_7, and 5 ms for the glassy samples. For ZrP_2O_7, the spinning frequency was 12 kHz and 70 t_1 increments, with 32 transients each, were collected using a recycle delay of 20 s. For the $PbO_x(P_2O_5)_{1-x}$ glasses, 64 t_1 increments, with 32 transients each, were recorded at 14 kHz spinning frequency using a recycle delay of 20 s. For all the samples, a presaturation sequence was applied to ensure equivalent conditions for each transient.

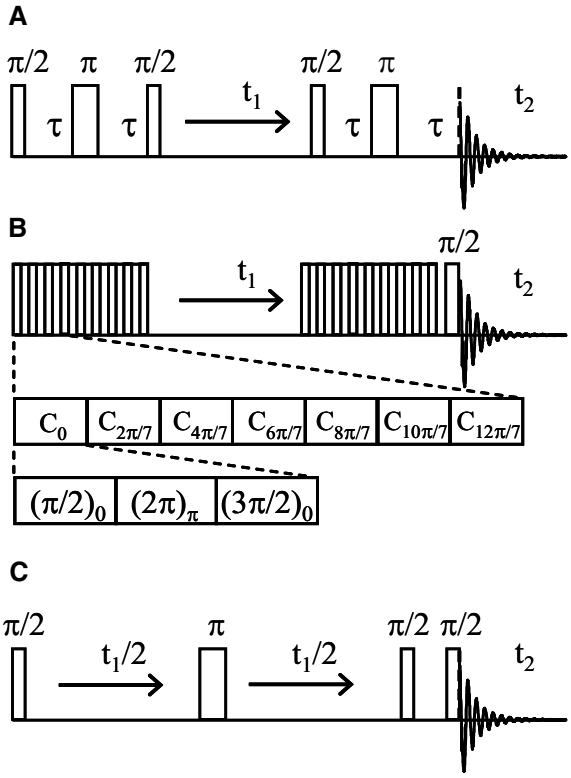

Fig. 1. (**a**) Refocused INADEQUATE pulse sequence [12] used for the 2D through-bond SQ–DQ correlation experiment; (**b**) POSTC7 pulse sequence [7] used for the 2D through-space SQ–DQ correlation experiment; (**c**) z-filtered spin-echo pulse sequence [26] used for the 2D J-resolved experiment.

The 2D ^{31}P through-space SQ–DQ MAS NMR correlation spectrum of ZrP_2O_7 was acquired at 10 kHz spinning frequency. The POSTC7 recoupling sequence [7] (Fig. 1b) was used to reintroduce the ^{31}P–^{31}P homonuclear dipolar interaction and to achieve the excitation and reconversion of double quantum coherences. The rf-field strength was ~70 kHz. Short excitation and reconversion periods of 600 μs were used. 80 t_1 increments, with 16 transients each, were collected using a recycle delay of 30 s and a presaturation sequence.

The 2D homonuclear J-resolved MAS NMR spectra were recorded using a z-filtered spin-echo sequence (Fig. 1c) [25–26]. The π/2 pulse duration was 2.3 μs. For the ZrP_2O_7 sample, the spinning frequency was 12 kHz and 64 t_1 increments with 32 transients each were collected using a recycle delay of 20 s. For the $PbO_x(P_2O_5)_{1-x}$ glasses, 70 t_1 increments, with 32 transients each, were recorded at 14 kHz spinning fre-

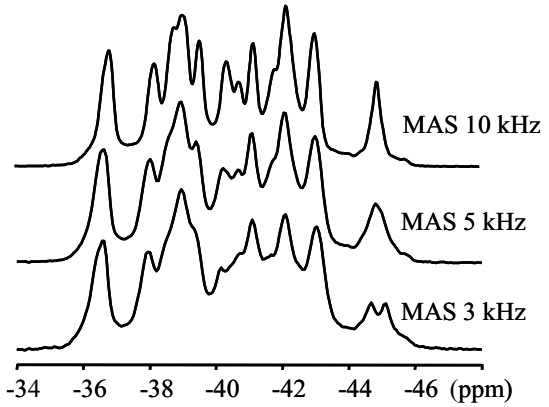

Fig. 2. ^{31}P MAS NMR spectra of ZrP_2O_7 recorded at spinning frequencies of 3, 5 and 10 kHz (isotropic region only).

quency, with a recycle delay of 20 s. In both cases, a presaturation sequence was applied to ensure equivalent conditions for each transient.

All the two-dimensional pure absorption phase spectra were obtained using a hypercomplex acquisition [27]. To avoid spinning sidebands in the ω_1 dimension, the t_1 time increment was synchronized with the rotor period. The spinning frequency was stabilized to ±10 Hz for all experiments. ^{31}P chemical shifts were referenced relative to 85% H_3PO_4 aqueous solution using the high-frequency positive convention. Simulations of the 1D MAS and 2D MAS correlation spectra were performed using the dmfit software [28].

3. Results and discussion

3.1. Space-group selection in MP_2O_7 crystalline compounds

The ^{31}P 1D MAS NMR spectra of ZrP_2O_7 obtained at different spinning rates are shown in Fig. 2 (isotropic region only). These spectra exhibit at least 13 partially overlapping ^{31}P isotropic resonances, indicating that the asymmetric unit of ZrP_2O_7 contains at least 13 crystallographically different P sites. This allows the exclusion of the possibility of a cubic symmetry with $Pa\bar{3}$ space group, for which only 11 independent phosphorus sites are expected. It can be noted that the positions and linewidths of these resonances vary to different extents with the spinning frequency. In particular, the single resonance located at –44.8 ppm for a spinning frequency of 10 kHz gives rise to a doublet at lower spinning rate, with a spinning-frequency-dependent splitting. Such unusual line shape effects have first been observed in ^{31}P MAS NMR spectra of homonuclear spin pairs with two chemically equivalent spins [29–32]. They are due to the ^{31}P–^{31}P homonuclear dipolar interaction, which lead to a second-order perturbation term in the average Hamiltonian, inversely proportional to the spinning frequency [29–32]. More recently, similar lineshape behaviours have been reported for P_2O_7 units with two inequivalent P sites having a weak isotropic chemical shift difference, as in the case of TiP_2O_7 [19] and $Cd_2P_2O_7$ [33].

As well as the number of individual ^{31}P sites, the number of P_2O_7 groups in the asymmetric unit can be used for space group assignment. To characterize the number of unique P_2O_7 groups in the ZrP_2O_7 structure, we have used the refocused INADEQUATE experiment, which allows determination of the through-bond P–O–P connectivities in crystalline and disordered phosphates [13]. The 2D ^{31}P through-bond SQ–DQ correlation MAS spectrum of ZrP_2O_7, obtained using the refocused INADEQUATE sequence [12], is depicted in Fig. 3. This 2D spectrum clearly exhibits 11 pairs of resolved cross-correlation peaks (A to K) that reflect the through-bond intra-P_2O_7 connectivity. The paired cross-peaks A show significantly broader linewidths and integrated intensities about three times higher than those of the remaining correlations (B to J), suggesting the presence of several overlapping contributions. In contrast, the paired cross-peaks K exhibit strongly reduced intensities, as expected from the overlap and the weak chemical shift difference of the coupled resonances. This 2D refocused INADEQUATE spectrum thus indicates that the room temperature structure of ZrP_2O_7 contains more than 11 P_2O_7 groups with two inequivalent P sites. This makes unlikely the possibility of $P2_13$ space group, for which only 11 P_2O_7 groups with two inequivalent P sites are expected and suggests that the most probable symmetry of ZrP_2O_7 is *Pbca*, which gives rise to 13 P_2O_7 groups with two inequivalent P sites. It should be remarked that, for *Pbca* symmetry, a single P_2O_7 groups with two crystallographically equivalent P sites related by a centre of inversion is also expected (see Table 1). Such P_2O_7 groups with two magnetically equivalent ^{31}P nuclei are not observable in a through-

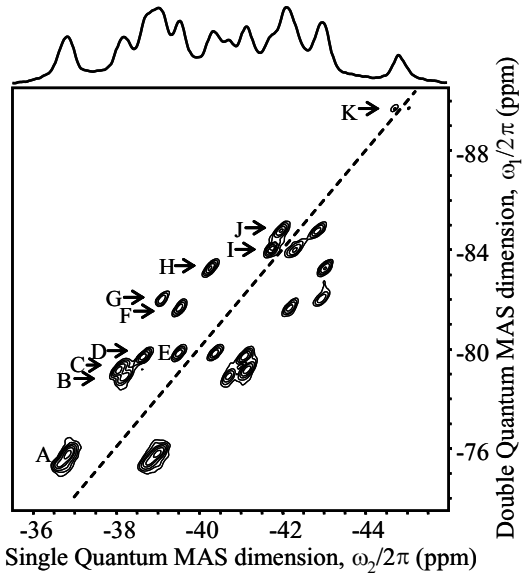

Fig. 3. ^{31}P 2D through-bond double quantum MAS correlation spectrum of ZrP_2O_7 obtained at 12 kHz spinning frequency using the refocused INADEQUATE experiment. The dashed line indicates the diagonal of the spectrum. The 1D MAS spectrum is shown above the 2D spectrum.

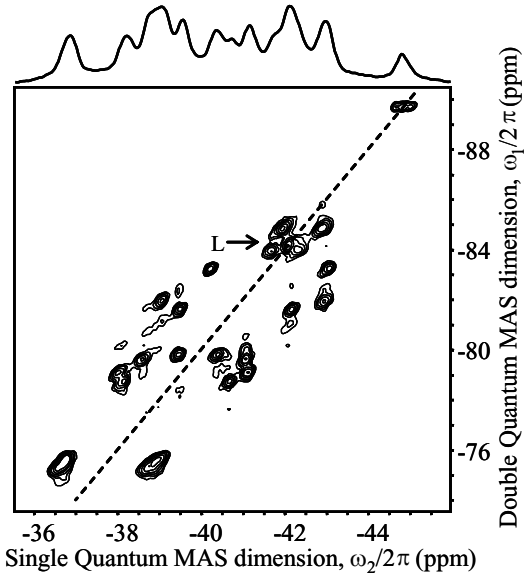

Fig. 4. ^{31}P 2D through-space double quantum MAS correlation spectrum of ZrP_2O_7 obtained using the POSTC7 sequence (10 kHz spinning frequency). The dashed line indicates the diagonal of the spectrum. The 1D MAS spectrum is shown above the 2D spectrum. Adapted from reference [34].

bond correlation spectrum, but they give rise to diagonal auto-correlation peaks in a through-space dipolar correlation spectrum. The 2D through-space SQ–DQ correlation spectrum of ZrP_2O_7 obtained using the POSTC7 sequence [7] is shown in Fig. 4 [34]. In addition to the 11 pairs of intense cross-correlation peaks characteristic of P_2O_7 groups with two inequivalent P sites previously/proved, this spectrum clearly shows a single intense auto-correlation peak along the diagonal (L), arising from a $P_2O_7^{4-}$ group containing two equivalent P sites. It should be noted that this spectrum, obtained using short excitation and reconversion periods, displays some additional correlation peaks of weaker intensities, due to the presence of weaker longer-range dipolar couplings. These weak-intensity peaks reflect the inter-P_2O_7 spatial proximities, providing additional structural information, but they can damage the spectral resolution in more complex cases [35]. Analysis of the peak intensities in Fig. 4 shows again that the paired cross-peaks A have approximately triple integrated intensities, suggesting the presence of three overlapping cross-correlation peaks corresponding to three $P_2O_7^{4-}$ groups. Good fits (not shown) of the quantitative 1D MAS and 2D correlation spectra were obtained with 27 distinct ^{31}P resonances of approximately equal intensity corresponding to 13 $P_2O_7^{4-}$ units (A to K) with two inequivalent P sites and one $P_2O_7^{4-}$ group (L) with two equivalent P sites. This indicates that the room temperature structure of ZrP_2O_7 adopts *Pbca* space-group symmetry, which requires 13 $P_2O_7^{4-}$ groups in general positions and one lying on an inversion centre.

As observed for other crystalline phosphates, the weak through-bond ^2J(P–P) coupling that drives the coherence transfer in the refocused INADEQUATE experiment is significantly smaller than the line width of the ^{31}P resonances and is not resolved in 1D MAS and 2D correlation spectra. This through-bond J coupling can be clearly proved from the 2D J-resolved experiment [25], which has been previously used to measure weak ^2J(P–P) couplings in metal phosphine complexes [9,36]. The 2D J-resolved MAS spectrum of ZrP_2O_7, recorded using a z-filtered spin-echo sequence [26], is depicted in Fig. 5. In this 2D spectrum, the characteristic doublets due to the weak ^2J(P–P) couplings are clearly resolved in the indirect ω_1 dimension and are correlated to the individual ^{31}P resonances in the ω_2 dimension. From the observed splitting, the magnitude of the intra-P_2O_7 ^2J(P–P) coupling constants is measured to range between 10 and 14 Hz. As

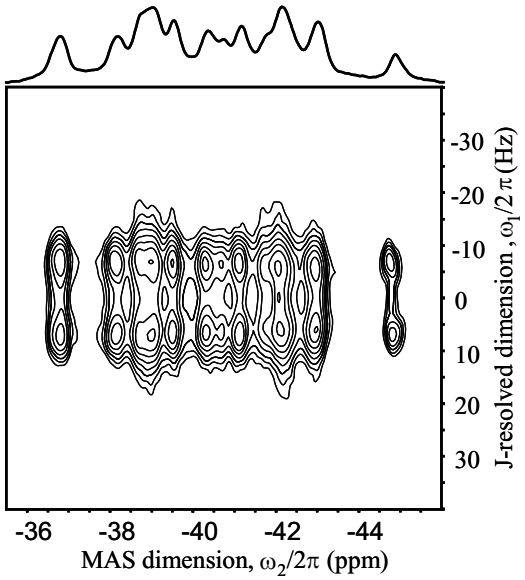

Fig. 5. ^{31}P 2D J-resolved MAS spectrum of ZrP_2O_7 recorded at 12 kHz spinning frequency using a *z*-filtered spin-echo sequence. The 1D MAS spectrum is shown above the 2D spectrum.

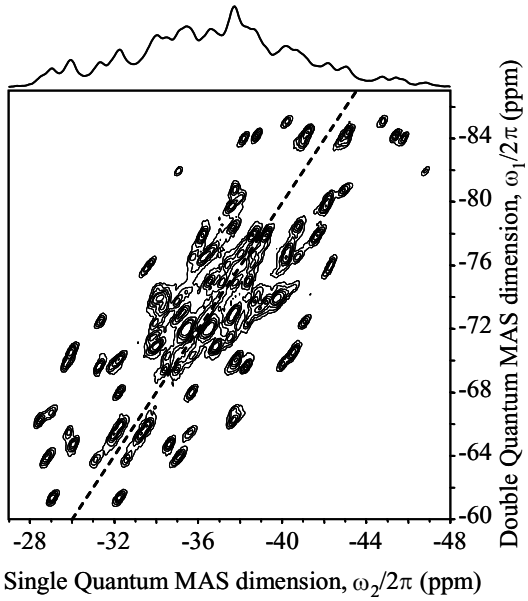

Fig. 6. ^{31}P 2D through-bond double quantum MAS correlation spectrum of SnP_2O_7 obtained using the refocused INADEQUATE experiment (10 kHz spinning frequency). The dashed line indicates the diagonal of the spectrum. The 1D MAS spectrum is shown above the 2D spectrum. Adapted from reference [35].

expected, the resonance associated with the P_2O_7 group with two P sites related by a centre of inversion (located at –42.1 ppm in the ω_2 dimension) gives rise to a single peak in the ω_1 dimension, since there is no observable *J*-coupling for magnetically equivalent spins. It should be mentioned that the magnitude of the coupling constant measured here is slightly smaller than those reported for other pyrophosphates which range between about 16 and 25 Hz [18,19,33,35,37] and that the absolute sign of the ^2J(P–P) coupling in P–O–P units is known to be negative [37].

The use of the through-bond SQ–DQ correlation NMR spectra for space-group selection in MP_2O_7 compounds has also been recently illustrated in more complex cases. As an example, the refocused INADEQUATE spectrum obtained for SnP_2O_7 [35] is shown in Fig. 6. This 2D spectrum clearly exhibits a spectacular gain in resolution relative to the 1D MAS spectrum, and shows 49 pairs of distinct cross-correlation peaks (some of them having significantly stronger intensities than others). In this case, this shows that the asymmetric unit contains at least 49 P_2O_7 units with two inequivalent P sites and suggests that the room-temperature structure of SnP_2O_7 is monoclinic, with $P2_1$ or *Pc* symmetry [35].

3.2. Through-bond connectivities in PbO_x–P_2O_5 glasses

The ^{31}P 1D MAS NMR spectra of the $PbO_x(P_2O_5)_{1-x}$ glasses ($x = 0.52, 0.59, 0.66$) are shown in Fig. 7. These MAS NMR spectra exhibit several broad isotropic resonances that can be attributed to the different types of PO_4 tetrahedra forming the glass network, corresponding to the ^{31}P isotropic chemical shift range in crystalline lead phosphates (Q^n units, with *n* the number of bridging oxygen atoms) [23]. In agreement with previous work [23,38], the MAS spectrum of the glass with $x = 0.52$ shows an intense isotropic peak at about –24 ppm, which corresponds to Q^2 middle-chain groups involved in long phosphate chains or cycles, and a weaker intensity peak at about –9 ppm assigned to Q^1 end-chain groups. As the PbO content increases up to $x = 0.65$, the intensity of the Q^1 resonance increases, indicating a progressive depolymerisation of the phosphate network with PbO addition. For the glass with $x = 0.66$, the MAS spectrum exhibits a third isotropic resonance at 1.4 ppm, indicating the presence of Q^0 units. For each Q^n unit, the broadening of the resonance comes from a large distri-

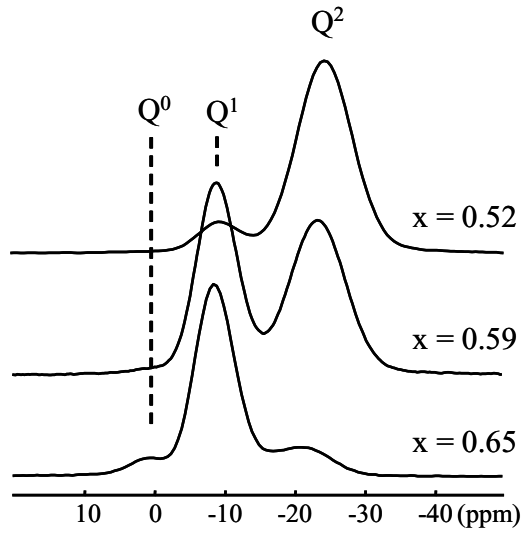

Fig. 7. ^{31}P MAS NMR spectra of the $PbO_x(P_2O_5)_{1-x}$ glasses recorded at a spinning frequency of 14 kHz (isotropic region only).

bution of ^{31}P chemical shifts that reflect the structural disorder in the glass, such as bond angles, bond-length variations and higher coordination-sphere disorder.

Although the quantitative analysis of these 1D MAS spectra provides a determination of the Q^n unit distribution as a function of the glass composition, information about pair connectivities between the Q^n units remains highly desirable for a better description of the disordered glassy network. Over the last few years, several homonuclear dipolar recoupling MAS NMR methods have been used to probe these Q^n pair connectivities [21–23]. These experiments allow the determination of nearest-neighbour spatial proximities between Q^n units in 2D through-space NMR correlation spectra, from which information about chemical connectivities is derived. A more convenient way to determine these Q^n connectivities is to use the weak through-bond ^{2}J(P-P) coupling. Through-bond homonuclear correlation NMR spectra have already been obtained in disordered solids [12,39] and we have recently shown that the refocused INADEQUATE experiment applies very efficiently to glassy phosphates [13].

The possibility of directly determining the P–O–P through-bond connectivities between Q^n units in disordered phosphate networks is clearly illustrated in Fig. 8, which shows the through-bond SQ–DQ correlation spectra of the $PbO_x(P_2O_5)_{1-x}$ glasses obtained using the refocused INADEQUATE experiment. These correlation spectra clearly show several broad correlation peaks that reflect the through-bond connectivities between the Q^n units. As shown in Fig. 8a, the refocused INADEQUATE spectrum of the glass with $x = 0.52$ exhibits an intense Q^2–Q^2 auto-correlation peak and Q^1–Q^2 cross-correlation peaks of weaker intensities, revealing the Q^2–Q^2 and Q^2–Q^1 connectivities involved in long phosphate chains. For the glass with $x = 0.59$, the 2D correlation spectrum shows the intense Q^1–Q^2 and Q^2–Q^2 correlations expected for phosphate chains of moderate length and an additional Q^1–Q^1 auto-correlation peak. This Q^1–Q^1 correlation peak gives evidence of the through-bond connectivity between two Q^1 end-chain units and is characteristic of P_2O_7 groups. This spectrum thus reveals the presence of a chain-length distribution in the glass network and confirms the results previously obtained from the interpretation of through-space dipolar correlation spectra [23]. It should be noted that, in a dipolar correlation experiment, the auto-correlation characteristic of P_2O_7 groups and the correlations between nearby (but not bonded) Q^1 groups of different chains overlap strongly, making the interpretation of the 2D spectrum more ambiguous. The 2D correlation spectrum of the glass with $x = 0.66$ is mainly composed of Q^1–Q^1 and Q^1–Q^2 correlations (Fig. 8c). As expected, the Q^0 resonance corresponding to isolated $[PO_4]^{3-}$ groups, for which there is clear evidence in the 1D MAS spectrum, is filtered out of the 2D through-bond correlation spectrum.

A notable feature revealed by these SQ–DQ through-bond correlation spectra is that the auto- and cross-correlation peaks of each Q^n unit appear at significantly different frequencies in the single-quantum dimension. For example, the centres of gravity of the broad auto- and cross-correlation peaks of the Q^1 resonance are located at about –8.4 and –9.7 ppm in the SQ dimension of the 2D maps. This was first observed from through-space dipolar correlation spectra [21–23] and suggests that the Q^n units linked to different types of PO_4 tetrahedra can be distinguished by their average isotropic chemical shift. As suggested by Witter et al. [22], the Q^n species are classified according to their connectivities, $Q^{n,ij}$, where the additional superscripts describe the type of the bonded PO_4 groups. Following this notation, the number of additional superscripts depends on n. For example, the Q^1 units forming P_2O_7 groups are labelled $Q^{1,1}$ and the Q^1

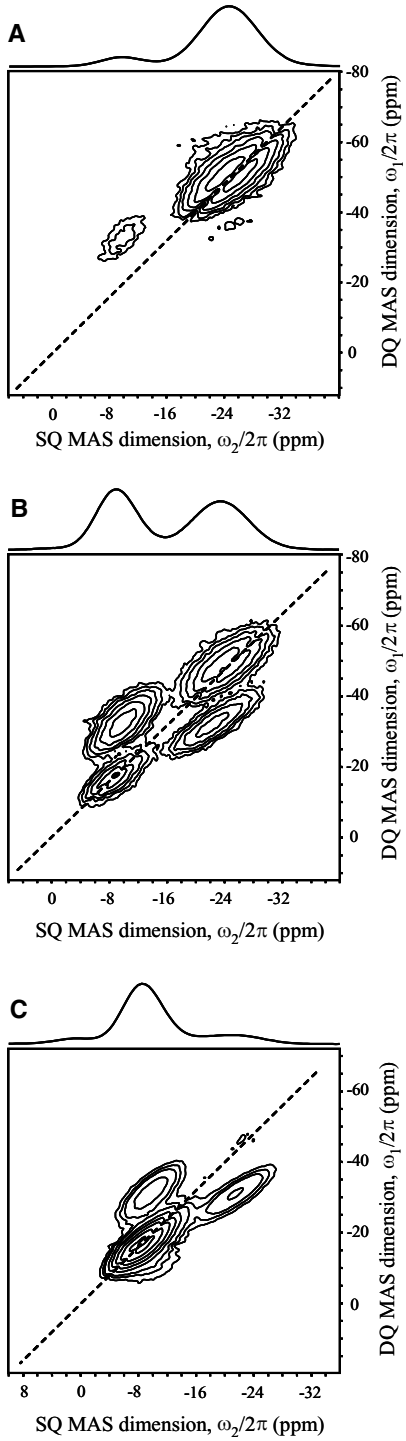

Fig. 8. ^{31}P 2D through-bond correlation MAS NMR spectra of the $PbO_x(P_2O_5)_{1-x}$ glasses obtained using the refocused INADEQUATE experiment (14 kHz spinning frequency): (**a**) $x = 0.52$, (**b**) $x = 0.59$, (**c**) $x = 0.66$. The dashed line indicates the diagonal of the 2D spectra. The 1D MAS spectra are shown above the 2D spectra.

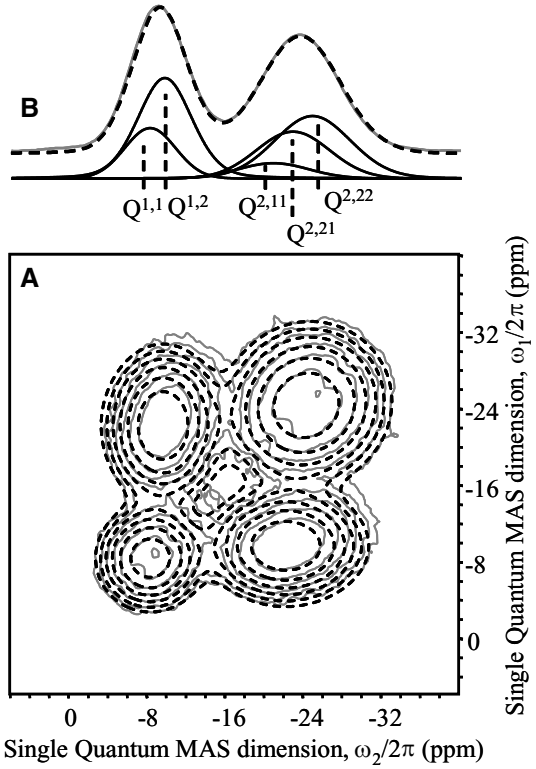

Fig. 9. (**a**) Sheared and symmetrized ^{31}P 2D refocused INADEQUATE spectrum of the $PbO_{0.59}(P_2O_5)_{0.41}$ glass and its simulation with the parameters reported in Table 2. (**b**) Fit of the quantitative ^{31}P MAS spectra with the $Q^{n,ij}$ contributions as determined from (**a**).

end-chain groups linked to Q^2 units are labelled $Q^{1,2}$, while a Q^2 group bonded to two Q^1 units (forming a trimer) is labelled $Q^{2,11}$. From the simulation of the 2D refocused INADEQUATE spectra, assuming a Gaussian line shape for each $Q^{n,ij}$ group, we have determined the ^{31}P isotropic chemical shifts and linewidths of the various $Q^{n,ij}$ units. To reduce the number of fitting parameters, the experimental SQ–DQ correlation spectra were sheared along the ω_1 dimension to obtain symmetric SQ–SQ correlation spectra with two equivalent dimensions [25]. The simulation of the 2D correlation spectrum obtained for the $PbO_{0.59}(P_2O_5)_{0.41}$ glass is shown in Fig. 9a. For each glass composition, the relative concentrations of the $Q^{n,ij}$ units were obtained from the fit of the quantitative 1D MAS spectrum (Fig. 9b), using the parameters determined from the 2D spectra and an additional intensity constraint, $[Q^{1,2}] = 2[Q^{2,11}] + [Q^{2,21}]$, required by the stoichiometry. The ^{31}P isotropic chemical shifts, linewidths and relative intensities of the $Q^{n,ij}$ groups obtained from these simulations are reported in Table 2. As pointed out previously [22], the phosphate chain-length distribution can be obtained from the $Q^{n,ij}$ concentrations for glasses with low P_2O_5 content.

As in the case of crystalline samples, the very weak isotropic ^2J(P–P) coupling used in the through-bond correlation experiment can be demonstrated using the 2D *J*-resolved experiment. As shown in Fig. 10a, the 2D *J*-resolved spectrum of the $PbO_{0.66}(P_2O_5)_{0.34}$ glass allows the clear resolution of characteristic multiplet patterns due to the ^2J(P–P) couplings. As expected, the Q^1 and Q^2 resonances are correlated in the indirect ω_1 dimension to doublet and triplet structures, respectively. A single resonance at zero-frequency is observed for the Q^0 resonance, since there is no ^2J(P–P) coupling. The cross-sections extracted along the indirect ω_1 dimension at the centres of gravity of the various Q^n resonances are depicted in Fig. 10b. Clearly, this 2D experiment provides an unambiguous attribution of the various Q^n resonances in glasses according to their *J*-multiplet structures and confirms the previous assignments based on the ^{31}P isotropic chemical shift range. Importantly, this 2D spectrum reveals a strong correlation between the distributions of ^{31}P isotropic chemical shifts and the distribution of ^2J(P–P) coupling constants of the Q^n resonances. We observe that, as the ^{31}P isotropic chemical shift varies from –6 to –11 ppm across the broad Q^1 resonance, the

Table 2
Isotropic ^{31}P chemical shifts (δ_{ISO}) and linewidths (full width at half-maximum: fwhm) of the $Q^{n,ij}$ units in the $PbO_x(P_2O_5)_{1-x}$ glasses obtained from the simulations of the 2D refocused INADEQUATE spectra ($\delta_{ISO} \pm 0.2$ ppm, fwhm ± 0.5 ppm). The relative intensities (I) of the $Q^{n,ij}$ units were obtained from the fit of the quantitative 1D MAS spectra using the same parameters ($I \pm 7\%$).

$Q^{n,ij}$ unit	Q^0	$Q^{1,1}$	$Q^{1,2}$	$Q^{2,11}$	$Q^{2,21}$	$Q^{2,22}$
δ_{ISO} (ppm),	1.4	–8.3	–9.7	–20.8	–22.8	–24.9
Fwhm (ppm)	6.2	6.2	6.6	8.5	8.8	9.2
Glass $Pb_{0.52}(P_2O_5)_{0.48}$, intensity (%)	—	—	11.0	—	11.0	78.0
Glass $Pb_{0.59}(P_2O_5)_{0.41}$, intensity (%)	—	14.0	31.5	6	19.5	29.0
Glass $Pb_{0.66}(P_2O_5)_{0.34}$, intensity (%)	5.5	52.0	27	11.5	4.0	—

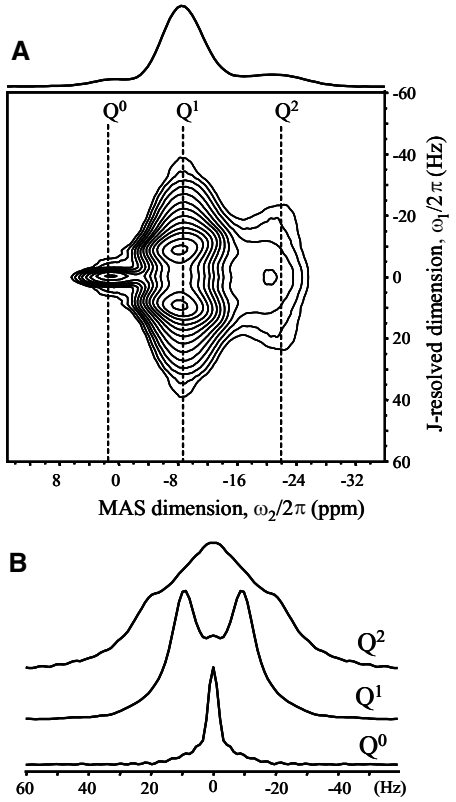

Fig. 10. (**a**) ^{31}P 2D J-resolved MAS spectrum of the $PbO_{0.66}(P_2O_5)_{0.34}$ glass recorded at 14 kHz spinning frequency using a *z*-filtered spin-echo sequence. The 1D MAS spectrum is shown above the 2D spectrum. (**b**) Cross sections of the 2D *J*-resolved spectrum at –22 ppm for the Q^2 units (top), at –8.7 ppm for the Q^1 units (middle) and at 1.4 ppm for the Q^0 units (bottom).

magnitude of the ^2J(P–P) coupling constants determined from the observed splitting increases continuously from 17 to 20.5 Hz. It should be noted that such a strong correlation between isotropic chemical shifts and *J*-coupling values is not observed for crystalline lead phosphates or for the MP_2O_7 compounds (see Fig. 5). Further experiments, allowing the measurement of the distributions of ^2J(P–P) coupling constants for each $Q^{n,ij}$ units from 3D NMR spectra, are in progress.

4. Conclusion

In this work, through-bond correlation NMR experiments have been used to characterize the structure of crystalline and disordered phosphates. In the case of MP_2O_7 crystalline compounds, we show that the refocused INADEQUATE experiment provides evidence of the number of distinct P sites and the number of P_2O_7 group in the asymmetric unit, allowing discrimination between the 12 possible space group symmetries of the room temperature structure. The results suggest that ZrP_2O_7 adopts the space group symmetry *Pbca* at room temperature. For lead phosphate glasses, we show that the refocused INADEQUATE experiment can be efficiently used to determine the P–O–P through-bond connectivities of the various Q^n units and to obtain intermediate-range order information in the disordered network. In these solids, the weak through-bond ^2J(P–P) couplings are clearly shown by using the 2D *J*-resolved experiment. For the lead phosphates glasses, this allows the assignment of the Q^n resonances according to their multiplet patterns. A strong correlation between the distribution of ^2J(P–P) couplings and the distribution of ^{31}P isotropic chemical shifts of the Q^n resonances is experimentally observed in these disordered systems.

Acknowledgements

FF, DM, IJK and RKH acknowledge support by European Community Contract HPRI-CT-1999-00042 and HPMT-CT-2000-00169. JSOE acknowledges support from the EPSRC under GR/N00524 and GR/M35222/01; RKH thanks the EPSRC for Grant GR/M88341.

References

[1] D.P. Raleigh, M.H. Levitt, R.G. Griffin, Chem. Phys. Lett. 146 (1988) 71.
[2] R. Tycko, G. Dabbagh, J. Am. Chem. Soc. 113 (1991) 9444.
[3] A.E. Bennett, J.H. Ok, R.G. Griffin, S. Vega, J. Chem. Phys. 96 (1992) 8624.
[4] M. Baldus, M. Tomaselli, B.H. Meier, R.R. Ernst, Chem. Phys. Lett. 230 (1994) 329.
[5] Y.K. Lee, N.D. Kurur, M. Elm, O.G. Johannessen, N.C. Nielsen, M.H. Levitt, Chem. Phys. Lett. 242 (1995) 304.
[6] M. Feike, D.E. Demco, R. Graf, J. Gottwald, S. Hafner, H.W. Spiess, J. Magn. Reson. A 122 (1996) 214.
[7] M. Hohwy, H.J. Jakobsen, M. Edén, M.H. Levitt, N.C. Nielsen, J. Chem. Phys. 108 (1998) 2686.
[8] C.A. Fyfe, Y. Feng, H. Gies, H. Grondey, G.T. Kokotailo, J. Am. Chem. Soc. 112 (1990) 3264.

[9] G. Wu, R.E. Wasylishen, Organometallics 11 (1992) 3242.
[10] M. Baldus, B.H. Meier, J. Magn. Reson. A 121 (1996) 65.
[11] A. Lesage, C. Auger, S. Caldarelli, L. Emsley, J. Am. Chem. Soc. 119 (1997) 7867.
[12] A. Lesage, M. Bardet, L. Emsley, J. Am. Chem. Soc. 121 (1999) 10987.
[13] F. Fayon, G. Le Saoût, L. Emsley, D. Massiot, Chem. Commun. (2002) 1702.
[14] K.R. Laud, F.A. Hummel, J. Am. Ceram. Soc. 54 (1971) 296.
[15] V. Korthuis, N. Khosrovani, A.W. Sleight, N. Roberts, R. Dupree, W.W. Warren, Chem. Mater. 7 (1995) 412.
[16] N. Khosrovani, V. Korthuis, A.W. Sleight, T. Vogt, Inorg. Chem. 35 (1996) 485.
[17] H. Vollenke, A. Wittmann, H. Novotny, Monatsh. Chemie 94 (1963) 956.
[18] R.J. Iuliucci, B.H. Meier, J. Am. Chem. Soc. 20 (1998) 9062.
[19] X. Helluy, C. Marichal, A. Sebald, J. Phys. Chem. B 104 (2000) 2836.
[20] S.W. Martin, Eur. J. Solid-State Inorg. Chem. 28 (1991) 163.
[21] M. Feike, C. Jäger, H.W. Spiess, J. Non-Cryst. Solids 223 (1998) 200.
[22] R. Witter, P. Hartmann, J. Vogel, C. Jäger, Solid-State NMR 13 (1998) 198.
[23] F. Fayon, C. Bessada, J.-P. Coutures, D. Massiot, Inorg. Chem. 38 (1999) 5212.
[24] A. Bax, R. Freeman, T.A. Frenkiel, J. Am. Chem. Soc. 103 (1981) 2102.
[25] R.R. Ernst, G. Bodenhausen, A. Wokaun, Principles of Nuclear Magnetic Resonance in One and Two Dimensions, Clarendon Press, Oxford, 1987.
[26] S.P. Brown, M. Pérez-Torralba, D. Sanz, R.M. Claramunt, L. Emsley, Chem. Commun. (2002) 1852.
[27] D.J. States, R.A. Haberkorn, D.J. Ruben, J. Magn. Reson. 48 (1982) 286.
[28] D. Massiot, F. Fayon, M. Capron, I.J. King, S. Le Calvé, B. Alonso, J.O. Durand, B. Bujoli, Z. Gan, G. Hoatson, Magn. Reson. Chem. 40 (2002) 70.
[29] M.M. Maricq, J.S. Waugh, J. Chem. Phys. 70 (1979) 3300.
[30] A. Kubo, C.A. McDowell, J. Chem. Phys. 92 (1990) 7156.
[31] K. Eichele, G. Wu, R.E. Wasylishen, J. Magn. Reson. A 101 (1993) 157.
[32] G. Wu, R.E. Wasylishen, J. Chem. Phys. 98 (1993) 6138.
[33] S. Dusold, J. Kümmerlen, A. Sebald, J. Phys. Chem. A 101 (1997) 5895.
[34] I.J. King, F. Fayon, D. Massiot, R.K. Harris, J.S.O. Evans, Chem. Commun. (2001) 1766.
[35] F. Fayon, I.J. King, R.K. Harris, R.K.B. Gover, J.S.O. Evans, D. Massiot, Chem. Mater 15 (2003) 2234.
[36] G. Wu, R.E. Wasylishen, Inorg. Chem. 31 (1992) 145.
[37] S. Dusold, W. Milius, A. Sebald, J. Magn. Reson. 135 (1998) 500.
[38] S. Prabhakar, K.J. Rao, C.N.R. Rao, Chem. Phys. Letters 139 (1987) 96.
[39] C.T.G. Knight, R.J. Kirkpatrick, E. Oldfield, J. Non-Cryst. Solids 116 (1990) 140.